www.sciencemag.org/content/347/6220/aaa0571/suppl/DC1

Supplementary Material for

Birth of a comet magnetosphere: A spring of water ions

Hans Nilsson,* Gabriella Stenberg-Wieser, Etienne Behar, Cyril Simon Wedlund, Herbert Gunell, Masatoshi Yamauchi, Rickard Lundin, Stas Barabash, Martin Wieser, Chris Carr, Emanuele Cupido, Jim Burch, Andrei Fedorov, Jean-André Sauvaud, Hannu Koskinen, Esa Kallio, Jean-Pierre Lebreton, Anders Eriksson, Niklas Edberg, Ray Goldstein, Pierre Henri, Christoph Koenders, Prachet Mokashi, Zoltan Nemeth, Ingo Richter, Karoly Szego, Martin Volwerk, Claire Vallat, Martin Rubin

*Corresponding author. E-mail: hans.nilsson@irf.se

Published 23 January 2015, *Science* **347**, aaa0571 (2015)
DOI: 10.1126/science.aaa0571

This PDF file includes:

Supplementary Text

Instrument operations

RPC-ICA has not been operated continuously due to instrument safety concerns. Regular operations have been conducted from 15 May 2014. Water ions were first detected on 7 August 2014 and were subsequently observed on 11 and 17 August. After this only very brief periods with water ions were observed, until 21 September. On 21 September strong solar and comet activity allowed us to detect several phenomena as described in the main text. On 30 September we once again observed significant amounts of water ions as well as a strong and steady He^+ signal. Interspersed with observations of solar wind – comet interaction are periods with an apparently undisturbed solar wind also when Rosetta is close to the nucleus. This was for example observed on 23 September 2014.

Basic theory of the solar wind pick up process

To a first approximation the solar wind interaction with a thin comet atmosphere can be understood in terms of the effect on newborn ions from the electric ($\boldsymbol{E}_{sw}$) and magnetic ($\boldsymbol{B}_{sw}$) fields of the solar wind. These are related to the solar wind velocity ($\boldsymbol{U}_{sw}$) according to the relation

$$\boldsymbol{E}_{sw} + \boldsymbol{U}_{sw} \times \boldsymbol{B}_{sw} = 0$$

This is known as the "frozen-in" criterion, the solar wind magnetic field being frozen into the solar wind plasma. In the solar wind reference frame the electric field is zero. A newborn ion, stationary relative to the solar wind flow, will see an electric field $\boldsymbol{E}_{sw}$ induced by the solar wind. Note also that for the case of the magnetic field being parallel to the solar wind velocity there is no induced electric field, $\boldsymbol{U}_{sw} \times \boldsymbol{B}_{sw}$ is 0. The basic ion pick-up process is further described in *(4,5,16)*.

Ions moving in a magnetic field gyrate. A newborn ion has a velocity in the solar wind reference frame of typically 400 km/s. For a magnetic field of the order of 1 nT, as expected in the vicinity of 67P/Churyumov-Gerasimenko for the initial observations, this corresponds to a gyro radius for a water ion of the order of 10 000 km. Therefore one may expect that newborn ions with an energy of only a few 100 eV will move in the solar wind electric field direction.

Field of view of the instrument

RPC-ICA has a field of view of 360° in the central detector plane (see Fig. 3 for a schematic illustration). Electrostatic entrance deflection is used to bring in particles from approximately +/- 45° from this plane. For sectors 10 to 15 and 0 and negative elevation angles the spacecraft body blocks the field of view (see *(12)* for details).

The energy table we are using has been in-flight adjusted so that the lowest energy ions we observe (and which are also observed by RPC-IES) have an energy close to zero. In flight investigation of on board monitor values for the high voltages confirm the adjustment to the energy table, which also brought the alpha particle to proton energy per

charge ratio closer to 2 on average. This gives a sparse energy sampling at low energies. The observed fluxes could thus be underestimates. Furthermore, due to the shift in the energy table, there is a mismatch between the energy table and the entrance elevation setting. The observed ions for a given setting have lower energy than expected. The voltage applied to achieve a certain elevation angle is thus too high, leading to a too high elevation angle. Therefore ions at energies below about 1 keV have a higher elevation angle than intended. For the lowest energy, ions can enter the instrument only for a setting close to 0°.

Therefore RPC-ICA can only observe the coldest water ions for certain favorable conditions. Water ions may therefore be more common than we have observed. The negative spacecraft potential in a relatively dense plasma helps the situation, as it accelerates the plasma towards the instrument. Cold plasma is, despite the negative spacecraft potential, only observed coming from one direction. Thus the plasma is accelerated, but the net flux should not be much influenced by the negative spacecraft potential (see below).

In the main paper we only indicated the directions where we observed ions using a schematic picture. For completeness, we summarize the sectors in which the different plasma components were observed in table S1.

Calculation of ENA fluxes

On 30-09-2014, RPC-ICA detected He^+ ions in combination with the expected solar wind He^{2+}. He^+ was observed also on 21 September, which is our sample of a day with increased solar wind and comet activity, but the signal was very weak. On 30 September when Rosetta was 20 km from the center of the comet nucleus, RPC-ICA observed a strong and steady He^+ signal. We show an energy–mass matrix from this day in Fig. S1. From this average data we determine the relative flux of He^+ to He^{2+} to be 2.1% on this day.

He^+ may be produced from charge exchange between the solar wind and the neutral environment of the comet. The main production channel within 100 km of the comet nucleus is assumed to be $He^{2+} + H_2O \rightarrow He^+ + X$, with X being H_2O^+or fragment ions, with a cross section of $8.4\times10^{-20}m^2$ at 0.83 keV/amu of collision energy, corresponding to a solar wind speed of 400 km s^{-1} *(22)*. Other channels (involving O and H) can be ignored since the density of the corresponding neutrals is low in comparison to water H_2O.

The density of solar wind alpha particles (He^{2+}) at the position $\mathbf{r} = (x,y,z)$ is given by:

$$N_\alpha(\mathbf{r}) = N_\alpha^{\mathrm{SW}} e^{-\sigma_\alpha I(\mathbf{r})} \quad (1)$$

where N_a^{sw} is the density of alpha particles colliding with neutrals N_n (H_2O) on their path to the detector. The charge-exchange cross section σ_α is assumed constant since the ions are considered to have a beam-like structure of constant energy in the $\mathbf{r}$ direction. The water column density $I(\mathbf{r})$ is defined as:

$$I(\mathbf{r}) = I(x,y,z) = \int_x^\infty N_n(\mathbf{r}')\, dx' \quad \text{with} \quad |\mathbf{r}'| = \sqrt{x'^2 + y^2 + z^2} \quad (2)$$

Here the x-axis points from the center of the comet towards the sun, forming a Cartesian coordinate system together with y and z.

One can derive an analytical expression for $I(\mathbf{r})$ in the case where the analyzed point of the x-axis points from the center of a spherical nucleus to the Sun. By conservation of matter,

$$N_{\mathrm{He}^+}(\mathbf{r}) = N_\alpha^{\mathrm{SW}} - N_\alpha(\mathbf{r}) = N_\alpha^{\mathrm{SW}}\left(1 - e^{-\sigma_\alpha I(\mathbf{r})}\right) \quad (3)$$

The energy loss of He^{2+} ion is small compared with its initial energy (~ 4 keV) and, therefore, the velocity of a newly born He^+ ion, U_{He^+}, is about the same as the velocity of the initial He^{2+} ion, U_α. The ratio of ion fluxes can in this case be derived analytically by:

$$R = \frac{N_{\mathrm{He}^+}(\mathbf{r})\, U_{\mathrm{He}^+}}{N_\alpha(\mathbf{r})\, U_\alpha} = \frac{N_{\mathrm{He}^+}(\mathbf{r})}{N_\alpha(\mathbf{r})} = \frac{1 - e^{-\sigma_\alpha I(\mathbf{r})}}{e^{-\sigma_\alpha I(\mathbf{r})}} \quad (4)$$

From this equation, the column density can be estimated:

$$I(\mathbf{r}) = \frac{\ln(R+1)}{\sigma_\alpha} \sim \frac{R}{\sigma_\alpha} \quad \text{for} \quad R << 1 \quad (5)$$

The numerical application on 30-09-2014 at the time of RPC-ICA's observation and at a distance r_0 = 18 km from the comet nucleus surface, yields, for an observed He^+/He^{2+} flux ratio R = 0.021:

$I_{\mathrm{obs}}(r_0) = 2.5 \times 10^{17}\ \mathrm{m}^{-2}$ (6)

We also calculated an estimate of an equivalent outgassing rate Q, using a simple model that links Q with the atmospheric density N_{model}, assuming a spherically symmetric Haser-like profile *(23)* for the cometary neutral H_2O atmosphere:

$$N_{\mathrm{model}} = \frac{Q}{4\pi v_o \mathbf{r}^2} \quad (7)$$

where v_0 is the velocity of the outgassing material (H_2O). A conservative estimate of v_0 = 400 m s^{-1} was chosen (*e.g., 15*), which lies within the wide range of values measured by ROSINA-COPS (ROSINA team, pers. comm.).

Integrating N_{model} along the constant (y,z) line according to equation (2) results in a modelled column density, $I_{\mathrm{model}}(\mathbf{r})$, with only one unknown, Q:

$$I_{\mathrm{model}}(\mathbf{r}) = \frac{Q}{4\pi v_o} \int_x^\infty \frac{1}{x'^2 + y^2 + z^2}\, dx' \quad (8)$$

From equations (6) and (8), at the position of RPC-ICA where a ratio of 2.1% was measured, we estimate an equivalent outgassing rate:

$$Q_{\mathrm{eq}} = \frac{4\pi v_o I_{\mathrm{obs}}(r_0)}{\int_{x_0}^\infty \frac{1}{x'^2 + y_0^2 + z_0^2}\, dx'} \quad (9)$$

The numerical application gives $Q_{\mathrm{eq}} \sim 1.4 \times 10^{25}\ \mathrm{s}^{-1}$. This corresponds in turn to an estimated H_2O density of about $1 \times 10^{13}\ \mathrm{m}^{-3}$, a value lying in the lower limit of ROSINA/COPS measurements for the same day (ROSINA team, pers. comm.), hence validating *a posteriori* our approach.

Calculation of hydrogen ENA flux

The flux of energetic neutral hydrogen atoms H_{ENA} can be derived in a similar fashion as He^+ ions, i.e., through the charge-exchange reaction:

$$H_{sw}^+ + H_2O \rightarrow H_{ENA} + H_2O^+$$

The local H/H^+ cometary ratio at the position of the spacecraft is obtained by using the column density I_{obs} in equation (5) and replacing σ_α with the cross section for the charge exchange between protons and water molecules, $\sigma_H = 1.8\times10^{-19}$ m^2 *(24)*, valid around 1 keV impact energy. The corresponding H/H^+ ratio is then:

$$R(H/H^+) = 0.044 \quad (10)$$

which is more than twice the He^+/He^{2+} ratio.

Using the equivalent Q_{eq} value calculated above in the expression of the column density inferred at the surface of the comet, the propagated near-surface H/H^+ ratio at the terminator is estimated at 0.33, about 8 times the ratio deduced at Rosetta's position.

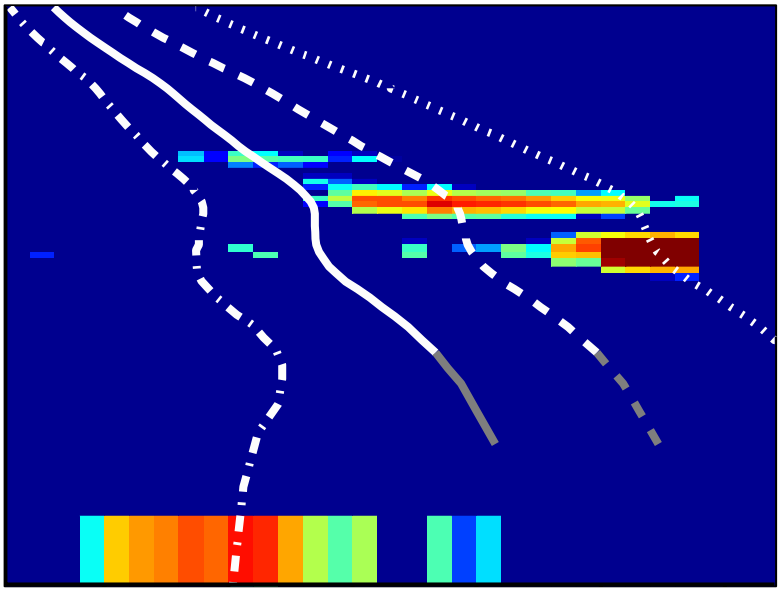

Fig. S1.

Energy-mass matrix from 30 September, 18:00 to 20:00 UT . The white lines show the calibrated position of the peak of the signal for ions with mass 1 amu/e (dotted), 2 amu/e (dashed), 4 amu/e (solid) and 16 amu/e (dash-dotted), respectively. H^+, He^{2+} and He^+ are seen at about 1, 2 and 4 keV. Cometary ions are seen at 10 eV. Grey lines show extrapolation beyond the laboratory calibration. The line at mass about 16 amu/e has been determined through in-flight calibration.

Time	Distance to the sun	Distance to the comet	Solar wind H^+ ~1 amu/e	Solar wind He^{2+} ~2 amu/e	Water ions 12 – 24 amu/e	Accelerated comet ions 12 – 24 amu/e
2014-08-07, 00:20 – 04:40 UT	**3.6 AU**	**100 km**	**11**	**11**	**7**	
2014-08-11, 13:40 – 14:47 UT	**3.6 AU**	**92 km**	**11**		**7**	
2014-09-21, 14:50 – 21:53 UT	**3.3 AU**	**30.9 km**	**8-9**	**9**	**5 – 7 (mainly 6)**	**12**
2014-09-30, 17:02 – 20:20 UT	**3.3 AU**	**19.9 km**	**9**	**9**	**5 - 6**	

Table S1.

Sectors where different ion species / populations were detected, corresponding to different angles of arrival. The sector numbers are defined in Fig. 3.

References and Notes

1. K. Altwegg, H. Balsiger, J. Geiss, Composition of the volatile material in Halley's coma from in situ measurements. *Space Sci. Rev.* **90**, 3–18 (1999). doi:10.1023/A:1005256607402

2. T. Mukai, W. Miyake, T. Terasawa, M. Kitayama, K. Hirao, Plasma observation by Suisei of solar-wind interaction with comet Halley. *Nature* **321** (6067s), 299–303 (1986). doi:10.1038/321299a0

3. F. M. Neubauer, Giotto magnetic field results on the boundaries of the pile-up region and the magnetic cavity. *Astron. Astrophys.* **187**, 73–79 (1987).

4. K. I. Gringauz, T. I. Gombosi, A. P. Remizov, I. Apáthy, I. Szemerey, M. I. Verigin, L. I. Denchikova, A. V. Dyachkov, E. Keppler, I. N. Klimenko, A. K. Richter, A. J. Somogyi, K. Szegő, S. Szendrő, M. Tátrallyay, A. Varga, G. A. Vladimirova, First in situ plasma and neutral gas measurements at comet Halley. *Nature* **321** (6067s), 282–285 (1986). doi:10.1038/321282a0

5. A. J. Coates, Ionospheres and magnetospheres of comets. *Adv. Space Res.* **20**, 255–266 (1997). doi:10.1016/S0273-1177(97)00543-7

6. M. Rubin, C. Koenders, K. Altwegg, M. R. Combi, K.-H. Glassmeier, T. I. Gombosi, K. C. Hansen, U. Motschmann, I. Richter, V. M. Tenishev, G. Tóth, Plasma environment of a weak comet—Predictions for Comet 67P/Churyumov–Gerasimenko from multifluid-MHD and hybrid models. *Icarus* **242**, 38–49 (2014). doi:10.1016/j.icarus.2014.07.021

7. K. Szegö *et al*., Physics of mass loaded plasmas. *Space Sci. Rev.* **94**, 429–671 (2000). doi:10.1023/A:1026568530975

8. I. Ribas, E. F. Guinan, M. Gudel, M. Audard, Evolution of the solar activity over time and effects on planetary atmospheres. I. High-energy irradiances (1-1700 Å). *Astrophys. J.* **622**, 680–694 (2005). doi:10.1086/427977

9. J. G. Luhmann, The solar wind interaction with unmagnetized planets: A tutorial. *Geophys. Monogr.* **58**, 401–411 (1991).

10. R. Reinhard, The Giotto encounter with comet Halley. *Nature* **321** (6067s), 313–318 (1986). doi:10.1038/321313a0

11. A. Johnstone, A. Coates, S. Kellock, B. Wilken, K. Jockers, H. Rosenbauer, W. Studemann, W. Weiss, V. Formisano, E. Amata, R. Cerulli-Irelli, M. Dobrowolny, R. Terenzi, A. Egidi, H. Borg, B. Hultquist, J. Winningham, C. Gurgiolo, D. Bryant, T. Edwards, W. Feldman, M. Thomsen, M. K. Wallis, L. Biermann, H. Schmidt, R. Lust, G. Haerendel, G. Paschmann, Ion flow at comet Halley. *Nature* **321** (6067s), 344–347 (1986). doi:10.1038/321344a0

12. C. Carr, E. Cupido, C. G. Y. Lee, A. Balogh, T. Beek, J. L. Burch, C. N. Dunford, A. I. Eriksson, R. Gill, K. H. Glassmeier, R. Goldstein, D. Lagoutte, R. Lundin, K. Lundin, B. Lybekk, J. L. Michau, G. Musmann, H. Nilsson, C. Pollock, I. Richter, J. G. Trotignon, RPC: The Rosetta plasma consortium. *Space Sci. Rev.* **128**, 629–647 (2007). doi:10.1007/s11214-006-9136-4

13. H. Nilsson, R. Lundin, K. Lundin, S. Barabash, H. Borg, O. Norberg, A. Fedorov, J.-A. Sauvaud, H. Koskinen, E. Kallio, P. Riihelä, J. L. Burch, RPC-ICA: The ion composition analyzer of the Rosetta plasma consortium. *Space Sci. Rev.* **128**, 671–695 (2007). doi:10.1007/s11214-006-9031-z

14. A. J. Coates, A. D. Johnstone, D. E. Huddleston, B. Wilken, K. Jockers, H. Borg, E. Amata, V. Formisano, M. B. Bavassano-Cattaneo, J. D. Winningham, C. Gurgiolo, F. M. Neubauer, Pickup water group ions at comet Grigg-Skjellerup. *Geophys. Res. Lett.* **20**, 483–486 (1993). doi:10.1029/93GL00174

15. A. Eriksson, R. Boström, R. Gill, L. Åhlén, S.-E. Jansson, J.-E. Wahlund, M. André, A. Mälkki, J. A. Holtet, B. Lybekk, A. Pedersen, L. G. Blomberg, RPC-LAP: The Rosetta Langmuir probe instrument. *Space Sci. Rev.* **128**, 729–744 (2007). doi:10.1007/s11214-006-9003-3

16. H. Balsiger, K. Altwegg, P. Bochsler, P. Eberhardt, J. Fischer, S. Graf, A. Jäckel, E. Kopp, U. Langer, M. Mildner, J. Müller, T. Riesen, M. Rubin, S. Scherer, P. Wurz, S. Wüthrich, E. Arijs, S. Delanoye, J. D. Keyser, E. Neefs, D. Nevejans, H. Rème, C. Aoustin, C. Mazelle, J.-L. Médale, J. A. Sauvaud, J.-J. Berthelier, J.-L. Bertaux, L. Duvet, J.-M. Illiano, S. A. Fuselier, A. G. Ghielmetti, T. Magoncelli, E. G. Shelley, A. Korth, K. Heerlein, H. Lauche, S. Livi, A. Loose, U. Mall, B. Wilken, F. Gliem, B. Fiethe, T. I. Gombosi, B. Block, G. R. Carignan, L. A. Fisk, J. H. Waite, D. T. Young, H. Wollnik, Rosina – Rosetta orbiter spectrometer for ion and neutral analysis. *Space Sci. Rev.* **128**, 745–801 (2007). doi:10.1007/s11214-006-8335-3

17. Materials and methods, and calculation of energetic neutral atom (ENA) fluxes, are provided as supplementary materials on *Science* Online.

18. E. Kallio, S. Barabash, K. Brinkfeldt, H. Gunell, M. Holmström, Y. Futaana, W. Schmidt, T. Säles, H. Koskinen, P. Riihelä, R. Lundin, H. Andersson, M. Yamauchi, A. Grigoriev, J. D. Winningham, R. A. Frahm, J. R. Sharber, J. R. Scherrer, A. J. Coates, D. R. Linder, D. O. Kataria, J. Kozyra, J. G. Luhmann, E. Roelof, D. Williams, S. Livi, P. C. Brandt, C. C. Curtis, K. C. Hsieh, B. R. Sandel, M. Grande, M. Carter, J.-A. Sauvaud, A. Fedorov, J.-J. Thocaven, S. McKenna-Lawler, S. Orsini, R. Cerulli-Irelli, M. Maggi, P. Wurz, P. Bochsler, N. Krupp, J. Woch, M. Fränz, K. Asamura, C. Dierker, Energetic Neutral Atoms (ENA) at Mars: Properties of the hydrogen atoms produced upstream of the martian bow shock and implications for ENA sounding technique around non-magnetized planets. *Icarus* **182**, 448–463 (2006). 10.1016/j.icarus.2005.12.019 doi:10.1016/j.icarus.2005.12.019

19. M. Hässig *et al*., Time variability and heterogeneity in the coma of 67P/Churyumov-Gerasimenko. *Science*.

20. M. H. Rees, *Physics and Chemistry of the Upper Atmosphere* (Cambridge Univ. Press, 1989).

21. K. C. Hansen, T. Bagdonat, U. Motschmann, C. Alexander, M. R. Combi, T. E. Cravens, T. I. Gombosi, Y.-D. Jia, I. P. Robertson, The plasma environment of comet 67P/Churyumov-Gerasimenko throughout the Rosetta main mission. *Space Sci. Rev.* **128**, 133–166 (2007). doi:10.1007/s11214-006-9142-6

22. J. B. Greenwood, R. J. Mawhorter, I. Cadez, J. Lozano, S. J. Smith, A. Chutjian, The contribution of charge exchange to extreme ultra-violet and x-ray astronomy. *Phys. Scr. T* **110**, 358–363 (2004). doi:10.1238/Physica.Topical.110a00358

23. L. Haser, Distribution d'intensité dans la tête d''une comète. *Bull. Soc. Roy. Sci. Liège* **43**, 740-750 (1957).

24. B. G. Lindsay, D. R. Sieglaff, K. A. Smith, R. F. Stebbings, Charge transfer of 0.5-, 1.5-, and 5-keV protons with H_2O: Absolute differential and integral cross sections. *Phys. Rev. A* **55**, 3945–3946 (1997). doi:10.1103/PhysRevA.55.3945